JAERI-M
83-164

ATOMIC STRUCTURE CALCULATION OF ENERGY LEVELS AND OSCILLATOR STRENGTHS IN Ti ION, II

(3s-3p AND 3p-3d TRANSITIONS in Ti X)

October 1983

Keishi ISHII*

日本原子力研究所
Japan Atomic Energy Research Institute

JAERI-M レポートは，日本原子力研究所が不定期に公刊している研究報告書です。
入手の問合わせは，日本原子力研究所技術情報部情報資料課（〒319—11 茨城県那珂郡東海村）あて，お申しこしください。なお，このほかに財団法人原子力弘済会資料センター（〒319-11 茨城県那珂郡東海村日本原子力研究所内）で複写による実費領布をおこなっております。

JAERI-M reports are issued irregularly.
Inquiries about availability of the reports should be addressed to Information Section, Division of Technical Information, Japan Atomic Energy Research Institute, Tokai-mura, Naka-gun, Ibaraki-ken 319-11, Japan.

編集兼発行　日本原子力研究所
印　　刷　山田軽印刷所

JAERI-M 83-164

Atomic Structure Calculation of Energy Levels and Oscillator Strengths in Ti Ion, II

(3s - 3p and 3p - 3d transitions in Ti X.)

Keishi ISHII*

(Received September 16,1983)

Energy levels and oscillator strengths are calculated for 3s-3p and 3p-3d transition arrays in Ti X, isoelectronic to Al I. The energy levels are obtained by the Slater-Condon theory of atomic structure, including explicitly the strong configuration interactions. The results are presented both in numerical tables and in diagrams. In the tables, the observed data are included for comparison, where available. The calculated weighted oscillator strengths (*gf*-value) are also displayed in figures, where the weighted oscillator strengths are plotted as a function of wavelength.

Keywords: Ti X, Highly Ionized Atom, Wavelength, Energy Level, Oscillator Strength, Plasma Diagnostic, Cowan Program

---

This work is partly supported by a research contract of Japan Atomic Energy Research Institute with Kyoto University in fiscal year 1983. This work is herewith published for its value to scientific community.

* Department of Engineering Science, Kyoto University, Kyoto 606

JAERI-M 83-164

Tiイオンのエネルギー準位と振動子強度の計算・II
(Ti Xの3s－3pおよび3p－3d遷移)

石 井 慶 之*

(1983年9月16日受理)

核融合プラズマにおける不純物問題解明のために必要とされる金属イオンの分光学的データに関する研究の一環として，Ti Xのエネルギー単位および$\Delta n = 0$，$n = 2 - 2$遷移の波長と振動子強度の理論計算を行った。計算にはHartree－XR波動関数とSlater－Condon理論に基づいたCowanプログラムを用いた。結果は表および図としてまとめた。文献調査による実験値は参考として表中に示した。

本報告は昭和58年度日本原子力研究所との協力研究の成果の一部である。

*京都大学工学部物理工学教室　京都市左京区吉田本町

Contents

目　　次

§ 1. INTRODUCTION

Knowledge of atomic structure in multiply charged ions, particularly of the structural material of the interior of the fusion devices, is important in the interpretation of spectral data from high temperature plasmas. The allowed $\Delta n=0$, $n=2-2$ transitions have been widely studied. The existing data have been compiled and published for the energy levels and the transition wavelengths[1] , and for the oscillator strengths[2,3] . Theoretical calculations are now available[4,5] , too. However, data on the $\Delta n=0$, $n=3-3$ transitions in M-shell are scarcer than those in L-shell, in spite of that the possible $\Delta n=0$ transitions in M-shell are much more abundant than those in L-shell.

The Ti X, a member of Al I-isoelectronic sequence has been studied by Edlén[6] in 1936, by Fawcett and Peacock[7] , by Svensson and Ekberg[8] , by Ekberg and Svensson[9] and by Fawcett[10] . Smitt *et al.*[11] have improved the accuracy of the previous measurements by examining closely the recorded spectrograms again and by studying the intervals in the ground configuration $3s^2 3p$ along the isoelectronic sequence. The configurations dealt with in the above all works are $3s^2 3p$, $3s3p^2$ and 3s3p3d. In 1971, Fawcett presented an extensive tabulation of wavelengths and classification for transitions in M-shell[12] .

Following the previous work on Ti IX[13] , the calculated energy levels of the lower lying seven of the nine possible configurations of the general type $3s^k 3p^q 3d^r$ $(k+q+r=3)$ in Ti X, and the wavelengths and the oscillator strenghts for the electric dipole transitions among them are presented. The calculated energy levels and wavelengths are listed and compared with the

observed ones, where available. The present gf-values are compared with other calculations, too. The calculated energy levels are also illustrated in diagrams. The calculated gf-values are plotted as a function of wavelength as well. The plotted line pattern may provide the helpful guidance to identify the missing lines. No experimental data are available at present for oscillator strengths and lifetimes.

§ 2. METHOD OF CALCULATION

The method of calculation used in the present work is the same as in the previous work on Ti IX[13]. Thus, only a brief description is given here. It consists of three steps. The first step is to calculate the radial integral values of the average energy of the configuration (E_{av}), the Slater radial integral (F^k, G^k), the spin-orbit integrals (ζ) and the configuration interaction integrals (R^k) by using the *ab initio* Hartree-XR wavefunctions[14,15].

The second step involves the adjustment of the radial parameters (E_{av}, F^k, G^k, ζ and R^k) by means of the least-squares optimization in order to minimize the differences between the computed and the observed energy levels. Strong configuration interactions are included explicitly.

The third step is to calculate the wavelengths and the weighted oscillator strengths (gf-values) for the electric dipole transitions between the configurations considered above. The programs used in the second and the third steps are also originally developed by Cowan[14-16]. A full explanation of this semi-empirical procedure is described by Wybourne[17], Bromage[18]

observed ones, where available. The present gf-values are compared with other calculations, too. The calculated energy levels are also illustrated in diagrams. The calculated gf-values are plotted as a function of wavelength as well. The plotted line pattern may provide the helpful guidance to identify the missing lines. No experimental data are available at present for oscillator strengths and lifetimes.

§ 2. METHOD OF CALCULATION

The method of calculation used in the present work is the same as in the previous work on Ti IX[13]. Thus, only a brief description is given here. It consists of three steps. The first step is to calculate the radial integral values of the average energy of the configuration (E_{av}), the Slater radial integral (F^k, G^k), the spin-orbit integrals (ζ) and the configuration interaction integrals (R^k) by using the *ab initio* Hartree-XR wavefunctions[14,15].

The second step involves the adjustment of the radial parameters (E_{av}, F^k, G^k, ζ and R^k) by means of the least-squares optimization in order to minimize the differences between the computed and the observed energy levels. Strong configuration interactions are included explicitly.

The third step is to calculate the wavelengths and the weighted oscillator strengths (gf-values) for the electric dipole transitions between the configurations considered above. The programs used in the second and the third steps are also originally developed by Cowan[14-16]. A full explanation of this semi-empirical procedure is described by Wybourne[17], Bromage[18]

and Cowan[19].

The configurations considered in the present work are grouped into the following two sets according to the parity:

First $3s^2 3p(\mathfrak{A}) + 3p^3(\mathfrak{B}) + 3s3p3d(\mathfrak{C})$

Second $3s3p^2(\mathfrak{A}) + 3s^2 3d(\mathfrak{B}) + 3p^2 3d(\mathfrak{C}) + 3s3d^2(\mathfrak{D})$.

The seven of the possible nine configurations of the general type $3s^k 3p^q 3d^r$ $(k+q+r=3)$ are considered and the configuration interactions in each parity are explicitly included in the present calculation. The remaining two configurations are excluded for being lying too highly.

§ 3. RESULTS

The first step calculation gives the *ab initio* values of the single configuration integrals and configuration interaction integrals as shown in the second column "HXR" of Tables 1 and 3. In the second step calculation, the optimization was reduced to manageable size by fixing ratio of F^k, G^k, ζ and R^k in each integrals[20-22]. The accuracy of the optimization was measured by the following quantities defined as

$$\Delta = \left[\sum_i (E_{calc}(i) - E_{obs}(i))^2 / (N_l - N_p)\right]^{1/2} , \qquad (1)$$

$$\sigma = \left[\sum_i (E_{calc}(i) - E_{obs}(i))^2 / N_l\right]^{1/2} , \qquad (2)$$

where $E_{calc}(i)$ and $E_{obs}(i)$ are i-th calculated and observed

and Cowan[19].

The configurations considered in the present work are grouped into the following two sets according to the parity:

First $3s^2 3p(\mathfrak{A}) + 3p^3(\mathfrak{B}) + 3s3p3d(\mathfrak{C})$

Second $3s3p^2(\mathfrak{A}) + 3s^2 3d(\mathfrak{B}) + 3p^2 3d(\mathfrak{C}) + 3s3d^2(\mathfrak{D})$.

The seven of the possible nine configurations of the general type $3s^k 3p^q 3d^r$ $(k+q+r=3)$ are considered and the configuration interactions in each parity are explicitly included in the present calculation. The remaining two configurations are excluded for being lying too highly.

§ 3. RESULTS

The first step calculation gives the *ab initio* values of the single configuration integrals and configuration interaction integrals as shown in the second column "HXR" of Tables 1 and 3. In the second step calculation, the optimization was reduced to manageable size by fixing ratio of F^k, G^k, ζ and R^k in each integrals[20-22]. The accuracy of the optimization was measured by the following quantities defined as

$$\Delta = \left[\sum_i (E_{calc}(i) - E_{obs}(i))^2 / (N_l - N_p)\right]^{1/2} , \qquad (1)$$

$$\sigma = \left[\sum_i (E_{calc}(i) - E_{obs}(i))^2 / N_l\right]^{1/2} , \qquad (2)$$

where $E_{\mathrm{calc}}(\mathrm{i})$ and $E_{\mathrm{obs}}(\mathrm{i})$ are i-th calculated and observed

levels, respectively, N_ℓ is the number of observed energy levels and N_p is the number of adjustable parameters. The following five kinds of free parameters were used in the optimization:

one average energy E_{av}
one scale factor for F^k
one scale factor for G^k
one scale factor for ζ
two scale factors for R^k.

The reduced electric dipole radial integrals obtained from the same *ab initio* HXR wavefunctions were utilized in the third step calculation combined with the second step results. In the following Tables and Figures, we closely maintain the format of our previous work on Ti IX[13].

3.1 *Configurations* $3s^2 3p$(Ⓐ), $3p^3$ (Ⓑ) *and* 3s3p3d(Ⓒ) *of the first parity*

Two ^2P levels of ground configuration $3s^2 3p$ are well established[11]. On the other hand, no doublet levels have been observed in $3p^3$ and 3s3p3d configurations. One ^4S level of $3p^3$ and three ^4D levels of 3s3p3d have reasonably been determined by extrapolation[9] along isoelectronic sequence, where the some energy levels of quartet terms reletive to ground doublet are known for Al I to Ar VI. The absolute position of quartet terms in Ti X, thus, may have some uncertainty, because of the nature of extrapolation. Accordingly, the least-squares-fit calculation was performed for the second parity configuratin at first,

whereby the uncertainty x was estimated as described below. Then, taking the x into account, the optimization procedure was applied to the first parity configuration, in which the adjustable parameters are grouped into the following two sets:

(1) $E_{av}(\mathfrak{A})$, $E_{av}(\mathfrak{B})$ and $E_{av}(\mathfrak{C})$,

(2) F^k, G^k and ζ_{nl}.

When parameters in one set were adjusted, those in the other were fixed. Two R^k were always fixed to the scaled values by the factor determined in 3.2. The optimization was repeated successively. The fitted parameter values are given in the column "Fitted", and the ratio of "Fitted" to "HXR" in Table 1. Whereas the difference between "Fitted" and "HXR" is given for E_{av}. The *std* deviation σ is $0.068\times10^3\,cm^{-1}$, which gives 0.011% of total energy range of the configurations ($\mathfrak{A}+\mathfrak{B}+\mathfrak{C}$).

The calculated and observed energy levels are listed in Table 2 for the $3s^2 3p$, $3p^3$ and 3s3p3d, together with their differences ("C-O"). The level designations and its percentage compositions in LS-basis are also given. The corresponding energy level dagram is shown in Fig.1. The percentage compositions are listed from the largest two contributions in the same configuration and one from the other when over about 10%. Table 2 shows that the average LS-purity is 76%. The level designation in the column "Term" is given by the most significant component, except a few levels, *e.g.* 504.341 and 501.792 levels in configuration $\mathfrak{C}$. Although their LS-purity is less than 50%, they are labeled as $^4D_{1/2}$ and $^4P_{1/2}$, respectivly, by considering the

smooth grouping of levels as shown in Fig.1. One can notice that there are several levels whose LS-purity is a little over 50%. Two pairs of ($3p^3\ ^2P$, $3s3p3d\ ^2P$) and ($3p^3\ ^2D$, $3s3p3d\ ^2D$) are considerably perturbed with strong mutual configuration interaction. For example, $3p^3\ ^2D$ has a 30% $3s3p3d\ ^2D$ character. One can notice further that the appreciable mixing occurs only among the levels with the same multiplicity. This makes it difficult to cause the intercombination transitions.

3.2 *Configurations* $3s3p^2$ (Α), $3s^2 3d$ (Β), $3p^2 3d$ (Ε) *and* $3s3d^2$ (Δ) *of the second parity*

The least-squares optimization was performed for the $3s3p^2$ (Α) and $3s^2 3d$ (Β) configurations, in which seven observed doublet levels are included. Three observed levels of quartet terms are excluded because of uncertainty in their absolute value. The *rms* deviation Δ of $0.076 \times 10^3\ cm^{-1}$ was achieved, when assumed the uncertainty x=400 cm^{-1} . This yields to 0.041% of total energy level spread of configurations Α and Β. The Hartree-XR and fitted values are given in Table 3, together with their ratios. The calculated energy levels are given in Table 4, along with the principal percentage compositions in LS-coupling basis. The average LS-purity is as high as 93%. The ^2D in one configuration, however, has a 12% other configuration character. The observed energy levels are also included for comparison. The difference between the calculated and the observed energy levels are given, assuming x=400 cm^{-1} . The calculated energy levels are displayed graphically in Fig.2.

The energy levels of $3p^2 3d$ (Ε), and $3s3d^2$ (Δ) configurations

are obtained by adopting the scaled parameters shown below "adopted" in Table 3. The results are given numerically in Table 5, and are illustrated in Fig.3. None of the level listed in Table 5 has been observed thus far.

3.3 *Wavelengths and Oscillator Strengths*

The reduced electric dipole radial integrals were obtained from the *ab initio* Hatree-XR wavefunction (Table 12), and used in the third step calculation without scaling. The calculated wavelengths and the *gf*-values for $3s^2 3p - 3s3p^2$ and $3s^2 3p - 3s^2 3d$ transition arrays are listed in Table 6, and those for $3s3p^2 - 3p^3$ and $3s3p^2 - 3s3p3d$ in Table 7, respectively. In both Tables, the observed wavelengths are included for comparison, with the difference between the calculated and observed ones. The agreement of the calculated wavelengths with the observed ones is excellent. The difference is only 0.06% at the worst.

The intercombination transitions are listed in Tables 8 and 9, along with estimated *gf*-value. Table 8 contains the spin-forbidden multiplet $3s^2 3p\ ^2P - 3s3p^2\ ^4P$. This multiplet has been observed for Al I to Ar VI along the isoelectronic sequence, and utilized to fix the quartet position in Ti X by extrapolation[9] . The present calculation shows that the *gf*-value is smaller than 0.005 for Ti X. Table 9 gives another spin-forbidden transitions between excited configurations. The calculated *gf*-value is again so small that the lines are hardly observed.

The total number of possible electric dipole transitions among the configurations considered in the present work reaches

483, even when limited for $gf \geqq 0.005$. In Table 10, the transitions from highest lying two configurations, *i.e.* $3p^2 3d$ and $3s3d^2$, are excluded. This is because that these highly excited levels are in many cases less populated. The lines marked with † are tentative assignment, whose wavelength was taken from Table 2 of Svensson and Ekberg[8]. The theoretical spectrum was generated from Table 10, and shown in Fig.4, where the gf-values are plotted in a logarithmic scale as a function of wavelength. Eleven lines above 520Å were excluded. A line rich region from 288 to 308Å is enlarged and shown in Fig.5. Both Figures provide a helpful guidance for identification of missing lines by direct comparison with a recorded spectrogram. All the energy levels belonging to $3s3p^2$ and $3s^2 3d$ configurations are known. On the other hand, only a few quartet levels of $3p^3$ and 3s3p3d have been observed. The absolute values of calculated energy level of the latter two configurations may still contain uncertainty to some extent at present, although they are determind here consistently with the established doublet system in the second parity configuration. However, a small change of E_{av}'s has no significant influence on the relative positions of the levels and it just shifts them up or down slightly as a whole. The same is true for the wavelength. Consequently the line patterns in Fig.4 and 5 do not change their general feature either.

In Table 11, the calculated lifetimes for the excited configurations are tabulated. One can see that most of the levels has lifetimes of the order of 0.01 to 0.1 nsec and a few quartet levels are metastable. The data for $3s3p^2$ and $3s^2 3d$ configurations may especially provide practical help for the

future beam-foil lifetime measurement.

§ 4. DISCUSSION

The average LS-purity of the first excited configuration of $3s3p^2$ is as high as 94%, as shown in Table 4. On the other hand, the LS-purity of the levels of $3p^3$ and 3s3p3d configurations in the first parity ranges from 36% to 100%, and the average is 76%. The purities vary from level to level in one configuration, and some of them have heavy admixtures from different configurations.

As is seen in Table 6, all the lines are observed, and they are in good agreement with the calculated ones. Thus, the classification for $3s^2 3p - 3s3p^2$ and $3s^2 3p - 3s^2 3d$ transitions is essentially established.

For $3s3p^2 - 3s3p3d$ transition (Table 7.), two lines with fairly large gf-value are not yet observed. The present calculation may provide helpful guidance for finding these missing lines, together with the calculated spectrum shown in Fig.4 and 5. No line due to $3s^2 3d - 3s3p3d$ has been observed so far. Some of the transition have gf-value larger than 1.00, as is seen in Table 10. They are thus expected to be observed. Figures 4 and 5 may be useful when compared with the recorded spectrograms, although the apparent line intensity is dependent on conditions of a light source.

The radial energy integrals were adjusted from their *ab initio* Hartree-XR values, while the radial electric dipole integrals were not. Therefore, the gf-values of transition between levels, of which at least one is subject to strong configuration interaction, are less accurate. However, the

future beam-foil lifetime measurement.

§ 4. DISCUSSION

The average LS-purity of the first excited configuration of $3s3p^2$ is as high as 94%, as shown in Table 4. On the other hand, the LS-purity of the levels of $3p^3$ and 3s3p3d configurations in the first parity ranges from 36% to 100%, and the average is 76%. The purities vary from level to level in one configuration, and some of them have heavy admixtures from different configurations.

As is seen in Table 6, all the lines are observed, and they are in good agreement with the calculated ones. Thus, the classification for $3s^2 3p - 3s3p^2$ and $3s^2 3p - 3s^2 3d$ transitions is essentially established.

For $3s3p^2 - 3s3p3d$ transition (Table 7.), two lines with fairly large gf-value are not yet observed. The present calculation may provide helpful guidance for finding these missing lines, together with the calculated spectrum shown in Fig.4 and 5. No line due to $3s^2 3d - 3s3p3d$ has been observed so far. Some of the transition have gf-value larger than 1.00, as is seen in Table 10. They are thus expected to be observed. Figures 4 and 5 may be useful when compared with the recorded spectrograms, although the apparent line intensity is dependent on conditions of a light source.

The radial energy integrals were adjusted from their *ab initio* Hartree-XR values, while the radial electric dipole integrals were not. Therefore, the gf-values of transition between levels, of which at least one is subject to strong configuration interaction, are less accurate. However, the

relative gf-values are fairly reliable, because the dipole integrals have a very little influence on them. The absolute gf-values can be determined only after the lifetimes are measured. In this context, Table 9 may be helpful for practical purpose of lifetime measurement.

The author would like to express his sincere thanks to Dr. Robert D. Cowan for making his programs available, and to Dr. Jan O. Ekberg for his kindest help to make MT copies of the programs and for his valuable discussions regarding the application of the program to the present work. He owes his thanks to Drs. K. Ozawa, Y. Nakai and T. Shirai of Japan Atomic Energy Research Institute for their valuable comments and for their arrangement of the publication of the report. Thanks are also due to the members at the Data Processing Center of Kyoto University for their help in the computation by use of the FACOM M-380 computer.

REFERENCES

1) B.C. Fawcett: "Wavelengths and classifications of emission lines due to $2s^2 2p^n - 2s2p^{n+1}$ and $2s2p^{n+1} - 2p^{n+2}$ transitions, $Z \leqq 28$", Atomic Data and Nuclear Data Tables 16 (1975) 135-164.

2) M.W. Smith and W.L. Wiese: "Graphical representations of systematic trends of atomic oscillator strengths along isoelectronic sequences and new oscillator strengths derived by interpolation", Astrophys. J. Suppl. Ser. 196 (1971) 103-192.

3) K. Ishii: "Systematic trends of oscillator strengths and lifetimes for $\Delta n=0$, $n=2-2$ transitions in multiply charged ions along isoelectronic sequence", U.S.-Japan Seminar on Plasma Spectroscopy, Kyoto (1979) p.54.

4) B.C. Fawcett: "Theoretical oscillator strengths for $2s^2 2p^n - 2s2p^{n+1}$ and $2s2p^{n+1} - 2p^{n+2}$ transitions and for $2s^2 2p^n$ "forbidden" transitions, Be I, B I, C I, N I, O I series, $Z \leqq 26$", Atomic Data and Nuclear Data Tables 22 (1978) 473-489.

5) K.T. Cheng, Y.-K. Kim and J.P. Desclaux: "Electric dipole, quadrupole, and magnetic dipole transition probabilities of ions isoelectronic to the first-row atoms, Li through F", Atomic Data and Nuclear Data Tables 24 (1979) 111-189.

6) B. Edlén: "Mg I-ähnlich Spektren der Elementen Titan bis Cobalt, Ti XI, V XII, Cr XIII, Mn XIV, Fe XV und Co XVI", Z. Physik 103 (1936) 536-541.

7) B.C. Fawcett and N.J. Peacock: "Highly ionized spectra of the transition elements", Proc. Phys. Soc. 91 (1967) 973-975.

8) L.Å . Svensson and J.O. Ekberg: "Titanium vacuum-spark spectrum from 50 to 425 Å ", Ark. Fys. 40 (1969) 145-163.

9) J.O. Ekberg and L.Å . Svensson: "Analyses of the XUV spectra of K, Ca, Sc and Ti isoelectronic with P I, Si I and Al I", Physica Scripta 2 (1970) 283-297.

10) B.C. Fawcett: "Classification of the lower energy levels of highly ionized transition elements", J. Phys. B3 (1970) 1732-1741.

11) R. Smitt, L.Å . Svensson and M. Outled: "An experimental study of $3s^2 3p^n - 3s3p^{n+1}$ in the Cl I, S I, Si I and Al I isoelectonic sequences", Physica Scripta 13 (1976) 293-307.

12) B.C. Fawcett: "Wavelengths and classifications of emission lines due to $3s^2 3p^n - 3s3p^{n+1}$ $3s3p^{n+1} - 3s^2 3p^{n-1}3d$ and other n=3-3 transitions", Report ARU-R4, Culham laboratory, UK (1971).

13) K. Ishii: "Atomic structure calculation of energy levels and oscillator strengths in Ti ion. (I. 3s - 3p and 3p - 3d transitions in Ti IX)", JAERI-M 83-155 (Report of Japan Atomic Energy Research Institute, 1983).

14) R.D. Cowan: "Atomic self-consistent-field calculations using statistical approximations for exchange and correlation", Phys. Rev. 163 (1967) 54-61.

15) R.D. Cowan and D.C. Griffin: "Approximate relativistic corrections to atomic radial wavefunctions", J. Opt. Soc. Am. 66 (1976) 1010-1014.

16) R.D. Cowan: "Theoretical calculation of atomic spectra using digital computers", J. Opt. Soc. Am. 58 (1968) 808-818, and "Theoretical study of $p^m - p^{m-1}\ell$ spectra", *ibid.* 58 (1968) 924-933.

17) B.G. Wybourne: *Spectroscopic Properties of Rare Earths* (John Wiley & Sons, New York, 1965).

18) G.E. Bromage: "The Cowan-Zealot-Suite of computer programs for atomic structure", Report **AL-R-3**, Appleton Laboratory, UK (1978).

19) R.D. Cowan: *The Theory of Atomic Structure and Spectra* (Univ. Calif. Press, Berkley, 1981).

20) G.E. Bromage, R.D. Cowan and B.C. Fawcett: "Energy levels and oscillator strengths for $3s^2 3p^n - 3s^2 3p^{n-1} 3d$ transitions of Fe X and Fe XI", Physica Scripta **15** (1977) 177-182.

21) G.E. Bromage, R.D. Cowan and B.C. Fawcett: "Atomic structure calculations involving optimization of radial integrals: Energy levels and oscillator strengths for Fe XII and Fe XIII 3p-3d and 3s-3p transitions", Mon. Not. R. astr. Soc. **183** (1978) 19-28.

22) G.E. Bromage: "Atomic structure calculations: Energy levels and oscillator strengths for 3s-3p and 3p-3d transitions in nickel XII to XV and vanadium VII to X spectra", Astron. Astrophys. Suppl. Ser. **41** (1980) 79-83.

23) W.L. Wiese and J.R. Fuhr: "Atomic transition probabilities for scandium and titanium (A critical data compilation of allowed lines)", J. Phys. Chem. Ref. Data **4** (1975) 263-352.

Table 1 Energy parameter values for the first parity configurations. (𝔄):$3s^2 3p$ (𝔅):$3p^3$ (𝔈):3s3p3d

Parameter	HXR	Fitted	Fitted/HXR*	CI
$Eav(𝔄)$	0.000	12.347	(+12.347)	
$\zeta(3p)$	5.597	5.091	0.910	
$Eav(𝔅)$	447.906	458.245	(+10.339)	
$F^2(3p,3p)$	112.048	100.160	0.894	
$\zeta(3p)$	5.572	5.068	0.910	
$Eav(𝔈)$	514.006	527.687	(+13.681)	
$\zeta(3p)$	5.572	5.014	0.910	
$\zeta(3d)$	0.461	0.298	0.650	
$F^2(3p,3d)$	111.363	99.547	0.894	
$G^1(3s,3p)$	147.465	128.523	0.872	
$G^2(3s,3d)$	101.362	88.347	0.872	
$G^1(3p,3d)$	129.381	112.768	0.872	
$G^3(3p,3d)$	83.642	72.902	0.872	
$R^1(ss,pp)$	147.163	88.298	0.600	𝔄*𝔅
$R^1(sp,pd)$	135.443	81.266	0.600	𝔄*𝔈
$R^2(sp,pd)$	103.389	62.033	0.600	𝔄*𝔈
$R^1(sd,pp)$	135.271	120.391	0.890	𝔅*𝔈
σ		0.068		

*Values in parentheses are (Fitted)-(HXR).

Table 2 Calculated and observed energy levels of $3s^2 3p$ (𝔄), $3p^3$ (𝔅) and 3s3p3d (ℭ) configurations in the 1st parity.

Term	J	Energy (in 10^3 cm^{-1}) Calc.	Obs.	C-O*	Percentage Composition
$3s^2 3p$ (𝔄)					
^2P	1/2	0.000	0.000[a]	0.000	99%
	3/2	7.542	7.543[a]	−0.001	99%
$3p^3$ (𝔅)					
^4S	3/2	421.626	421.188+x[b]	−0.000	98%
^2D	5/2	411.073			69%, 30% ℭ(^3P)^2D
	3/2	410.054			68%, 30% ℭ(^3P)^2D
^2P	3/2	458.466			77%, 16% ℭ(^3P)^2P
	1/2	458.109			80%, 15% ℭ(^3P)^2P
3s3p3d (ℭ)					
(^3P)^4F	9/2	470.567			100%
	7/2	467.602			100%
	5/2	465.399			100%
	3/2	463.875			100%
(^3P)^4D	7/2	505.595	505.266+x[b]	−0.109	100%
	5/2	505.553	505.134+x[b]	−0.019	81%, 19%(^3P)^4P
	3/2	505.079	504.516+x[b]	0.125	61%, 39%(^3P)^4P
	1/2	504.341			36%, 64%(^3P)^4P
(^3P)^4P	5/2	499.214			79%, 19%(^3P)^4D
	3/2	500.585			61%, 38%(^3P)^4D
	1/2	501.792			36%, 64%(^3P)^4D
(^3P)^2F	7/2	549.900			71%, 29%(^1P)^2F
	5/2	544.049			70%, 29%(^1P)^2F
(^3P)^2D	5/2	522.720			52%, 29%(^1P)^2D 17% 𝔅 ^2D
	3/2	522.742			52%, 29%(^1P)^2D 18% 𝔅 ^2D
(^3P)^2P	3/2	588.510			83%, 15% 𝔅 ^2P
	1/2	590.438			83%, 13% 𝔅 ^2P
(^1P)^2F	7/2	600.632			70%, 29%(^1P)^2F
	5/2	602.056			70%, 29%(^3P)^2F
(^1P)^2D	5/2	622.859			69%, 18%(^3P)^2D 13% 𝔅 ^2D
	3/2	622.312			53%, 20%(^1P)^2P 10% 𝔅 ^2D
(^1P)^2P	3/2	619.200			74%, 16%(^1P)^2D
	1/2	619.502			91%, 7% 𝔅 ^2P

[a] Smitt *et al.* (1976), ref. 11).
[b] Ekberg and Svensson (1970), ref. 9).
* When assumed uncertainty x=0.438.

Table 3 Energy parameter values for the second parity configurations. (𝔄):$3s3p^2$ (𝔅):$3s^2 3d$ (ℭ):$3p^2 3d$ (𝔇):$3s3d^2$

Parameter	HXR	Fitted	Fitted/HXR*	CI
Eav(𝔄)	203.635	219.929	(+16.294)	
F^2 (3p,3p)	112.081	104.815	0.936	
ζ(3p)	5.572	5.184	0.913	
G^1 (3s,3p)	147.325	128.398	0.872	
Eav(𝔅)	328.577	336.169	(+7.592)	
ζ(3d)	0.461	0.269	0.584	
Δ		0.076		
		Adopted		
Eav(ℭ)	740.354	740.354	(+0.000)	
F^2 (3p,3p)	111.894	104.719	0.936	
ζ(3p)	5.551	5.165	0.930	
ζ(3d)	0.461	0.269	0.584	
F^2 (3p,3d)	111.108	103.984	0.936	
G^1 (3p,3d)	129.216	112.616	0.872	
G^3 (3p,3d)	83.451	72.730	0.872	
Eav(𝔇)	836.598	836.598	(+0.000)	
F^2 (3d,3d)	116.662	108.183	0.936	
F^4 (3d,3d)	75.070	70.257	0.930	
ζ(3d)	0.457	0.266	0.584	
G^2 (3s,3d)	100.944	87.976	0.872	
R^1 (pp,sd)	135.242	120.365	0.890	𝔄*𝔅
R^1 (sp,pd)	135.271	81.163	0.600	𝔄*ℭ
R^2 (sp,pd)	103.182	61.909	0.600	𝔄*ℭ
R^1 (pp,dd)	128.906	77.344	0.600	𝔄*𝔇
R^3 (pp,dd)	83.181	49.909	0.600	𝔄*𝔇
R^1 (ss,pp)	146.981	88.189	0.600	𝔅*ℭ
R^2 (sd,dd)	104.060	62.436	0.600	𝔅*𝔇
R^1 (sd,pp)	135.020	120.168	0.890	ℭ*𝔇

*Values in parentheses are (Fitted)-(HXR).

Table 4 Calculated and observed energy levels of $3s3p^2$ (Ⓐ) and $3s^2 3d$ (Ⓑ) configurations in the 2nd parity.

Term	J	Energy (in 10^3 cm^{-1}) Calc.	Obs.	C−O*	Percentage Composition
$3s3p^2$ (Ⓐ)					
^{4}P	5/2	165.189	164.764+x[a]	0.025	99%
	3/2	161.075	160.655+x[a]	0.020	100%
	1/2	158.206	157.850+x[a]	−0.044	99%
^{2}D	5/2	212.550	212.598[a]	−0.048	87%, 12% Ⓑ ^{2}D
	3/2	212.098	212.046[a]	0.052	87%, 12% Ⓑ ^{2}D
^{2}P	3/2	285.231	285.217[a]	0.014	98%
	1/2	281.030	281.044[a]	−0.014	92%, 6% ^{2}S
^{2}S	1/2	264.458	264.467[a]	−0.009	93%, 6% ^{2}P
$3s^2 3d$ (Ⓑ)					
^{2}D	5/2	345.875	345.856[b]	0.019	87%, 12% Ⓐ ^{2}D
	3/2	345.331	345.329[b]	0.002	87%, 12% Ⓐ ^{2}D

[a] Smitt *et al.* (1976), ref.11).
[b] Ekberg and Svensson (1970), ref.9).
* When assumed uncertainty x=0.400.

Table 5 Calculated energy levels of $3p^2 3d$ (𝔈) and $3s3d^2$ (𝔇) configuration in the 2nd parity. Energy in $10^3 cm^{-1}$.

Term	J	Energy	Percentage Compositin
$3p^2 3d$ (𝔈)			
$(^3P)^4F$	9/2	695.151	99%
	7/2	692.353	97%
	5/2	690.059	98%
	3/2	688.395	98%
$(^3P)^4D$	7/2	707.849	96%
	5/2	705.826	97%
	3/2	705.338	92%
	1/2	706.854	53%, 29% $(^3P)^2P$, 15% $(^1D)^2P$
$(^3P)^4P$	5/2	741.257	58%, 31% $(^1D)^2D$
	3/2	741.485	79%, 15% $(^1D)^2D$
	1/2	741.791	98%
$(^3P)^2F$	7/2	789.539	75%, 11% $(^1D)^2F$, 14% 𝔇 ^2F
	5/2	787.566	72%, 13% $(^1D)^2F$
$(^3P)^2D$	5/2	828.647	58%, 39% $(^1S)^2D$
	3/2	831.737	57%, 42% $(^1S)^2D$
$(^3P)^2P$	3/2	698.335	59%, 28% $(^1D)^2P$
	1/2	701.637	34%, 47% $(^3P)^4D$, 17% $(^1D)^2P$
$(^1D)^2G$	9/2	725.530	88%, 11% 𝔇 ^2G
	7/2	724.640	89%, 11% 𝔇 ^2G
$(^1D)^2F$	7/2	683.638	64%, 22% $(^3P)^2F$, 12% 𝔇 ^2F
	5/2	680.824	64%, 24% $(^3P)^2F$, 12% 𝔇 ^2F
$(^1D)^2D$	5/2	736.513	44%, 42% $(^3P)^4P$
	3/2	738.275	59%, 19% $(^3P)^4P$, 10% 𝔇 ^2D
$(^1D)^2P$	3/2	764.889	40%, 31% $(^3P)^2P$, 19% 𝔇 ^2P
	1/2	762.849	43%, 35% $(^3P)^2P$, 20% 𝔇 ^2P
$(^1D)^2S$	1/2	774.414	87%, 11% 𝔇 ^2S
$(^1S)^2D$	5/2	778.899	53%, 34% $(^3P)^2D$
	3/2	773.422	47%, 34% $(^3P)^2D$
$3s3d^2$ (𝔇)			
^4F	9/2	805.837	100%
	7/2	805.439	100%
	5/2	805.127	100%
	3/2	804.905	100%
^4P	5/2	827.999	100%
	3/2	827.777	100%
	1/2	827.636	100%
^2G	9/2	866.628	89%, 11% 𝔈$(^1D)^2G$
	7/2	866.570	89%, 11% 𝔈$(^1D)^2G$
^2F	7/2	900.996	74%, 22% 𝔈$(^1D)^2F$
	5/2	900.778	73%, 21% 𝔈$(^1D)^2F$
^2D	5/2	862.825	83%, 17% 𝔈$(^1D)^2D$
	3/2	862.768	82%, 16% 𝔈$(^1D)^2D$
^2P	3/2	926.437	73%, 25% 𝔈$(^1D)^2P$
	1/2	925.814	74%, 25% 𝔈$(^1D)^2P$
^2S	1/2	914.173	88%, 11% 𝔈$(^1D)^2S$

Table 6 Calculated and observed wavelengths with weighted oscillator strengths for $3s^2 3p(^2P) - 3s3p^2(^2P)$ and $3s^2 3p(^2P) - 3s^2 3d(^2D)$ transitions.

Transition		Wavelength (in Å)				
Term–Term	J – J	Calc.	Obs.	C–O	gf	gf^*
$3s^2 3p - 3s3p^2$						
$^2P - ^2D$	3/2–5/2	487.786	487.654[a]	0.132	0.2746	0.182
	3/2–3/2	488.862	488.971[a]	−0.109	0.0155	0.020
	1/2–3/2	471.479	471.574[a]	−0.095	0.1774	0.105
$^2P - ^2P$	3/2–3/2	360.115	360.133[b]	−0.018	1.8573	
	1/2–3/2	350.593	350.610[b]	−0.017	0.3822	
	3/2–1/2	365.646	365.628[b]	0.018	0.5191	
	1/2–1/2	355.833	355.815[b]	0.018	0.5510	
$^2P - ^2S$	3/2–1/2	389.231	389.237[a]	−0.006	0.1200	
	1/2–1/2	378.131	378.135[a]	−0.004	0.3272	
$3s^2 3p - 3s^2 3d$						
$^2P - ^2D$	3/2–5/2	295.566	295.584[b]	−0.018	2.4279	2.69
	3/2–3/2	296.043	296.04 *	0.00	0.2998	0.30
	1/2–3/2	289.577	289.579[b]	−0.002	1.3514	1.58

[a] Smitt *et al.* (1976), ref.11).
[b] Svensson and Ekberg (1970), ref.9).
[c] Fawcett (1971), ref.12).
* Wiese and Fuhr (1975), ref.23).

Table 7 Calculated and observed wavelengths with weighted oscillator strengths for a particular transition of $3s3p^2\ {}^4P - 3p^3\ {}^4S$ and $3s3p^2\ {}^4P - 3s3p3d\ {}^4D$.

Trannsition		Wavelength (in Å)			
Term–Term	J – J	Calc.	Obs.	C–O	gf
$3s3p^2 - 3p^3$					
${}^4P-{}^4S$	5/2–3/2	389.959	389.99[c]	−0.03	1.0869
${}^4P-{}^4S$	3/2–3/2	383.802	383.93[c]	−0.13	0.7365
${}^4P-{}^4S$	2/2–3/2	379.622	379.74[c]	−0.12	0.3727
$3s3p^2 - 3s3p3d$					
${}^4P-({}^3P){}^4D$	5/2–7/2	293.767	293.684[b]	0.083	3.2027
${}^4P-({}^3P){}^4D$	5/2–5/2	293.803	293.798[b]	0.005	1.4298
${}^4P-({}^3P){}^4D$	3/2–5/2	290.294	290.294[b]	0.000	0.7972
${}^4P-({}^3P){}^4D$	5/2–3/2	294.213			0.3875
${}^4P-({}^3P){}^4D$	3/2–3/2	290.695	290.815[b]	−0.120	0.9032
${}^4P-({}^3P){}^4D$	1/2–3/2	288.290	288.462[b]	−0.172	0.0664
${}^4P-({}^3P){}^4D$	3/2–1/2	291.320			0.5199
${}^4P-({}^3P){}^4D$	1/2–1/2	288.905			0.0742

[a,b,c] see footnote in Table 6.

Table 8 Calculated wavelengths (in Å) of intercombination resonance multiplet $3s^2 3p\ ^2P^o - 3s3p^2\ ^4P$. The gf-value is smaller than 0.005 for all components.

Term	J - J	Wavelength
$^2P-^4P$	3/2-5/2	634.33
	3/2-3/2	651.33
	1/2-3/2	620.83
	3/2-1/2	663.73
	1/2-1/2	632.09

Table 9 Calculated wavelengths (in Å) of intercombination transitions $3s3p^2 - 3p^3$ and $3s3p^2 - 3s3p3d$, with $gf \geqq 0.005$.

Transition	Term-Term	J - J	Wavelength	gf
$3s3p^2 - 3p^3$	$^4P - ^2P$	3/2-3/2	336.258	0.0088
$3s3p^2 - 3s3p3d$	$^2D - ^4D$	5/2-7/2	341.244	0.0087
	$^2D - ^4P$	5/2-5/2	348.840	0.0150
	$^2P - ^4S$	3/2-5/2	276.514	0.0093

Table 10 Calculated and observed wavelengths (in Å) with $gf \geqq 0.005$ for transitions $3s^2 3p - 3s3p^2$, $3s^2 3p - 3s^2 3d$, $3s3p^2 - 3p^3$, $3s3p^2 - 3s3p3d$ and $3s^2 3d - 3s3p3d$. Arranged in order of decreasing wavelength.

No	Energy (10^3 cm^{-1})	Configuration	Term	J – J	Calc	Obs	gf
1	285.230–410.054	$3s3p^2 - 3p^3$	$^2P - {}^2D$	3/2–3/2	801.133		0.0130
2	285.230–411.073	$3s3p^2 - 3p^3$	$^2P - {}^2D$	3/2–5/2	794.642		0.2004
3	281.030–410.054	$3s3p^2 - 3p^3$	$^2P - {}^2D$	1/2–3/2	775.050		0.1147
4	264.458–410.054	$3s3p^2 - 3p^3$	$^2S - {}^2D$	1/2–3/2	686.833		0.0168
5	285.230–458.109	$3s3p^2 - 3p^3$	$^2P - {}^2P$	3/2–1/2	578.442		0.0433
6	285.230–458.465	$3s3p^2 - 3p^3$	$^2P - {}^2P$	3/2–3/2	577.251		0.2729
7	345.875–522.720	$3s^2 3d - 3s3p3d$	$^2D - (^3P)^2D$	5/2–5/2	565.467		0.0783
8	281.030–458.109	$3s3p^2 - 3p^3$	$^2P - {}^2P$	1/2–1/2	564.720		0.1418
9	345.330–522.720	$3s^2 3d - 3s3p3d$	$^2D - (^3P)^2D$	3/2–5/2	563.730		0.0142
10	345.330–522.742	$3s^2 3d - 3s3p3d$	$^2D - (^3P)^2D$	3/2–3/2	563.661		0.0543
11	281.030–458.465	$3s3p^2 - 3p^3$	$^2P - {}^2P$	1/2–3/2	563.585		0.0109
12	264.458–458.109	$3s3p^2 - 3p^3$	$^2S - {}^2P$	1/2–1/2	516.394		0.0217
13	264.458–458.465	$3s3p^2 - 3p^3$	$^2S - {}^2P$	1/2–3/2	515.444		0.1405
14	212.549–410.054	$3s3p^2 - 3p^3$	$^2D - {}^2D$	5/2–3/2	506.318		0.0603
15	212.098–410.054	$3s3p^2 - 3p^3$	$^2D - {}^2D$	3/2–3/2	505.164		0.2307
16	345.875–544.049	$3s^2 3d - 3s3p3d$	$^2D - (^3P)^2F$	5/2–5/2	504.607		0.0281
17	212.549–411.073	$3s3p^2 - 3p^3$	$^2D - {}^2D$	5/2–5/2	503.718		0.4154
18	345.330–544.049	$3s^2 3d - 3s3p3d$	$^2D - (^3P)^2F$	3/2–5/2	503.224		0.1777
19	212.098–411.073	$3s3p^2 - 3p^3$	$^2D - {}^2D$	3/2–5/2	502.575		0.0353
20	345.875–549.900	$3s^2 3d - 3s3p3d$	$^2D - (^3P)^2F$	5/2–7/2	490.137		0.2829
21	7.542–212.098	$3s^2 3p - 3s3p^2$	$^2P - {}^2D$	3/2–3/2	488.862	488.971[a]	0.0155
22	7.542–212.549	$3s^2 3p - 3s3p^2$	$^2P - {}^2D$	3/2–5/2	487.786	487.654[a]	0.2746
23	0.000–212.098	$3s^2 3p - 3s3p^2$	$^2P - {}^2D$	1/2–3/2	471.479	471.574[a]	0.1774
24	285.230–522.720	$3s3p^2 - 3s3p3d$	$^2P - (^3P)^2D$	3/2–5/2	421.071		0.1102
25	285.230–522.742	$3s3p^2 - 3s3p3d$	$^2P - (^3P)^2D$	3/2–3/2	421.032		0.0235

Table 10 *Continued*

26	281.030–522.742	$3s3p^2$ – 3s3p3d	$^2P - (^3P)^2D$	1/2–3/2	413.715		0.0728
27	345.875–588.509	$3s^2 3d$ – 3s3p3d	$^2D - (^3P)^2P$	5/2–3/2	412.143		0.0133
28	345.330–588.509	$3s^2 3d$ – 3s3p3d	$^2D - (^3P)^2P$	3/2–3/2	411.220		0.0198
29	345.330–590.437	$3s^2 3d$ – 3s3p3d	$^2D - (^3P)^2P$	3/2–1/2	407.985		0.0322
30	212.549–458.465	$3s3p^2$ – $3p^3$	$^2D - ^2P$	5/2–3/2	406.643		0.5967
31	212.098–458.109	$3s3p^2$ – $3p^3$	$^2D - ^2P$	3/2–1/2	406.487		0.3576
32	212.098–458.465	$3s3p^2$ – $3p^3$	$^2D - ^2P$	3/2–3/2	405.898		0.0724
33	345.875–600.631	$3s^2 3d$ – 3s3p3d	$^2D - (^1P)^2F$	5/2–7/2	392.532		3.4304
34	345.875–602.055	$3s^2 3d$ – 3s3p3d	$^2D - (^1P)^2F$	5/2–5/2	390.350		0.1393
35	165.189–421.626	$3s3p^2$ – $3p^3$	$^4P - ^4S$	5/2–3/2	389.959	389.99[c]	1.0869
36	345.330–602.055	$3s^2 3d$ – 3s3p3d	$^2D - (^1P)^2F$	3/2–5/2	389.522		2.4589
37	7.542–264.458	$3s^2 3p$ – $3s3p^2$	$^2P - ^2S$	3/2–1/2	389.231	389.237[a]	0.1200
38	264.458–522.742	$3s3p^2$ – 3s3p3d	$^2S - (^3P)^2D$	1/2–3/2	387.171		0.0064
39	161.075–421.626	$3s3p^2$ – $3p^3$	$^4P - ^4S$	3/2–3/2	383.802	383.93[c]	0.7365
40	158.206–421.626	$3s3p^2$ – $3p^3$	$^4P - ^4S$	1/2–3/2	379.622	379.74[c]	0.3727
41	0.000–264.458	$3s^2 3p$ – $3s3p^2$	$^2P - ^2S$	1/2–1/2	378.131	378.135[a]	0.3272
42	345.875–619.200	$3s^2 3d$ – 3s3p3d	$^2D - (^1P)^2P$	5/2–3/2	365.865		1.5542
43	7.542–281.030	$3s^2 3p$ – $3s3p^2$	$^2P - ^2P$	3/2–1/2	365.646	365.628[b]	0.5191
44	345.330–619.200	$3s^2 3d$ – 3s3p3d	$^2D - (^1P)^2P$	3/2–3/2	365.137		0.0134
45	345.330–619.502	$3s^2 3d$ – 3s3p3d	$^2D - (^1P)^2P$	3/2–1/2	364.735		0.7985
46	345.875–622.312	$3s^2 3d$ – 3s3p3d	$^2D - (^1P)^2D$	5/2–3/2	361.747		0.0732
47	345.330–622.312	$3s^2 3d$ – 3s3p3d	$^2D - (^1P)^2D$	3/2–3/2	361.035		1.2198
48	345.875–622.859	$3s^2 3d$ – 3s3p3d	$^2D - (^1P)^2D$	5/2–5/2	361.032		1.6618
49	345.330–622.859	$3s^2 3d$ – 3s3p3d	$^2D - (^1P)^2D$	3/2–5/2	360.323		0.0694
50	7.542–285.230	$3s^2 3p$ – $3s3p^2$	$^2P - ^2P$	3/2–3/2	360.115	360.133[b]	1.8573
51	0.000–281.030	$3s^2 3p$ – $3s3p^2$	$^2P - ^2P$	1/2–1/2	355.833	355.815[b]	0.5510
52	0.000–285.230	$3s^2 3p$ – $3s3p^2$	$^2P - ^2P$	1/2–3/2	350.593	350.610[b]	0.3822
53	212.549–499.214	$3s3p^2$ – 3s3p3d	$^2D - (^3P)^4P$	5/2–5/2	348.840		0.0150
54	212.549–505.595	$3s3p^2$ – 3s3p3d	$^2D - (^3P)^4D$	5/2–7/2	341.244		0.0087
55	161.075–458.465	$3s3p^2$ – $3p^3$	$^4P - ^2P$	3/2–3/2	336.258		0.0088

Table 10 *Continued*

56	165.189–467.602	$3s3p^2$ – 3s3p3d	$^4P - (^3P)^4F$	5/2–7/2	330.673		0.0080
57	285.230–588.509	$3s3p^2$ – 3s3p3d	$^2P - (^3P)^2P$	3/2–3/2	329.729		0.3925
58	285.230–590.437	$3s3p^2$ – 3s3p3d	$^2P - (^3P)^2P$	3/2–1/2	327.646		0.0698
59	281.030–588.509	$3s3p^2$ – 3s3p3d	$^2P - (^3P)^2P$	1/2–3/2	325.225		0.0146
60	281.030–590.437	$3s3p^2$ – 3s3p3d	$^2P - (^3P)^2P$	1/2–1/2	323.198		0.3483
61	212.549–522.720	$3s3p^2$ – 3s3p3d	$^2D - (^3P)^2D$	5/2–5/2	322.403		2.1829
62	212.549–522.742	$3s3p^2$ – 3s3p3d	$^2D - (^3P)^2D$	5/2–3/2	322.380		0.1448
63	212.098–522.720	$3s3p^2$ – 3s3p3d	$^2D - (^3P)^2D$	3/2–5/2	321.935		0.2145
64	212.098–522.742	$3s3p^2$ – 3s3p3d	$^2D - (^3P)^2D$	3/2–3/2	321.912		1.4424
65	264.458–588.509	$3s3p^2$ – 3s3p3d	$^2S - (^3P)^2P$	1/2–3/2	308.593	308.408[†]	1.6293
66	264.458–590.437	$3s3p^2$ – 3s3p3d	$^2S - (^3P)^2P$	1/2–1/2	306.768		0.5446
67	212.549–544.049	$3s3p^2$ – 3s3p3d	$^2D - (^3P)^2F$	5/2–5/2	301.659		0.1200
68	212.098–544.049	$3s3p^2$ – 3s3p3d	$^2D - (^3P)^2F$	3/2–5/2	301.249		0.9581
69	285.230–619.200	$3s3p^2$ – 3s3p3d	$^2P - (^1P)^2P$	3/2–3/2	299.428		0.2874
70	165.189–499.214	$3s3p^2$ – 3s3p3d	$^4P - (^3P)^4P$	5/2–5/2	299.378		0.2709
71	285.230–619.502	$3s3p^2$ – 3s3p3d	$^2P - (^1P)^2P$	3/2–1/2	299.158		0.2321
72	165.189–500.585	$3s3p^2$ – 3s3p3d	$^4P - (^3P)^4P$	5/2–3/2	298.154		0.1084
73	285.230–622.312	$3s3p^2$ – 3s3p3d	$^2P - (^1P)^2D$	3/2–3/2	296.664		1.1414
74	212.549–549.900	$3s3p^2$ – 3s3p3d	$^2D - (^3P)^2F$	5/2–7/2	296.427		1.4490
75	285.230–622.859	$3s3p^2$ – 3s3p3d	$^2P - (^1P)^2D$	3/2–5/2	296.184		3.6845
76	7.542–345.330	$3s^2 3p$ – $3s^2 3d$	$^2P - {}^2D$	3/2–3/2	296.043	296.04 *	0.2998
77	161.075–499.214	$3s3p^2$ – 3s3p3d	$^4P - (^3P)^4P$	3/2–5/2	295.736	295.584[†]	1.3022
78	281.030–619.200	$3s3p^2$ – 3s3p3d	$^2P - (^1P)^2P$	1/2–3/2	295.709	295.584[†]	1.2007
79	7.542–345.875	$3s^2 3p$ – $3s^2 3d$	$^2P - {}^2D$	3/2–5/2	295.566	295.584[b]	2.4279
80	281.030–619.502	$3s3p^2$ – 3s3p3d	$^2P - (^1P)^2P$	1/2–1/2	295.445		0.3479
81	161.075–500.585	$3s3p^2$ – 3s3p3d	$^4P - (^3P)^4P$	3/2–3/2	294.542		0.0882
82	165.189–505.079	$3s3p^2$ – 3s3p3d	$^4P - (^3P)^4D$	5/2–3/2	294.213		0.3875
83	165.189–505.553	$3s3p^2$ – 3s3p3d	$^4P - (^3P)^4D$	5/2–5/2	293.803	293.798[b]	1.4298
84	165.189–505.595	$3s3p^2$ – 3s3p3d	$^4P - (^3P)^4D$	5/2–7/2	293.767	293.684[b]	3.2027
85	281.030–622.312	$3s3p^2$ – 3s3p3d	$^2P - (^1P)^2D$	1/2–3/2	293.013	293.033[†]	0.9532

Table 10 *Continued*

86	158.206–500.585	$3s3p^2$ – 3s3p3d	$^4P - (^3P)^4P$	1/2–3/2	292.074	291.958†	0.9970
87	161.075–504.340	$3s3p^2$ – 3s3p3d	$^4P - (^3P)^4D$	3/2–1/2	291.320		0.5199
88	158.206–501.792	$3s3p^2$ – 3s3p3d	$^4P - (^3P)^4P$	1/2–1/2	291.048		0.6828
89	161.075–505.079	$3s3p^2$ – 3s3p3d	$^4P - (^3P)^4D$	3/2–3/2	290.695	290.815[b]	0.9032
90	161.075–505.553	$3s3p^2$ – 3s3p3d	$^4P - (^3P)^4D$	3/2–5/2	290.294	290.294[b]	0.7972
91	0.000–345.330	$3s^2 3p$ – $3s^2 3d$	$^2P - ^2D$	1/2–3/2	289.577	289.579[b]	1.3514
92	158.206–504.340	$3s^2 3d$ – 3s3p3d	$^4P - (^3P)^4D$	1/2–1/2	288.905		0.0742
93	158.206–505.079	$3s^2 3d$ – 3s3p3d	$^4P - (^3P)^4D$	1/2–3/2	288.290	288.462[b]	0.0664
94	264.458–619.502	$3s3p^2$ – 3s3p3d	$^2S - (^1P)^2P$	1/2–1/2	281.655		0.1162
95	264.458–622.312	$3s3p^2$ – 3s3p3d	$^2S - (^1P)^2D$	1/2–3/2	279.444		0.0987
96	161.075–522.720	$3s3p^2$ – 3s3p3d	$^4P - (^3P)^2D$	3/2–5/2	276.514		0.0093
97	212.549–588.509	$3s3p^2$ – 3s3p3d	$^2D - (^3P)^2P$	5/2–3/2	265.986		0.0085
98	212.549–600.631	$3s3p^2$ – 3s3p3d	$^2D - (^1P)^2F$	5/2–7/2	257.677	258.008†	1.5958
99	212.549–602.055	$3s3p^2$ – 3s3p3d	$^2D - (^1P)^2F$	5/2–5/2	256.735		0.0711
100	212.098–602.055	$3s3p^2$ – 3s3p3d	$^2D - (^1P)^2F$	3/2–5/2	256.438	256.525†	1.1307
101	212.549–619.200	$3s3p^2$ – 3s3p3d	$^2D - (^1P)^2P$	5/2–3/2	245.911		0.0160

[a,b,c,*] see footnote in Table 6.
†Svensson and Ekberg (1969), ref.8), and see text.

Table 11 Calculated lifetimes (in nsec) of levels in the excited configurations.

Conf	Term	J	Energy	Lifetime*
$3s3p^2$	^4P	5/2	165.189	---
		3/2	161.075	---
		1/2	158.206	---
	^2D	5/2	212.550	7.80(-1)
		3/2	212.098	6.95(-1)
	^2P	3/2	285.231	3.44(-2)
		1/2	281.030	3.64(-2)
	^2S	1/2	264.458	9.73(-2)
$3s^2 3d$	^2D	5/2	345.875	3.24(-2)
		3/2	345.331	3.07(-2)
$3p^3$	^4S	3/2	421.626	4.07(-2)
	^2D	5/2	411.073	4.29(-1)
		3/2	410.054	4.32(-1)
	^2P	3/2	458.466	1.09(-1)
		1/2	458.109	1.06(-1)
3s3p3d	$(^3P)^4F$	9/2	470.567	---
		7/2	467.602	1.65(+1)
		5/2	465.399	---
		3/2	463.875	---
	$(^3P)^4D$	7/2	505.595	3.23(-2)
		5/2	505.553	3.46(-2)
		3/2	505.079	3.76(-2)
		1/2	504.341	4.27(-2)
	$(^3P)^4P$	5/2	499.214	4.99(-2)
		3/2	500.585	4.31(-2)
		1/2	501.792	3.72(-2)
	$(^3P)^2F$	7/2	549.900	6.79(-2)
		5/2	544.049	7.09(-2)
	$(^3P)^2D$	5/2	522.720	3.73(-2)
		3/2	522.742	3.73(-2)
	$(^3P)^2P$	3/2	588.510	2.83(-2)
		1/2	590.438	3.01(-2)
	$(^1P)^2F$	7/2	600.632	2.59(-2)
		5/2	602.056	2.54(-2)
	$(^1P)^2D$	5/2	622.859	1.63(-2)
		3/2	622.312	1.70(-2)
	$(^1P)^2P$	3/2	619.200	2.07(-2)
		1/2	619.502	2.14(-2)

Table 11 *Continued*

Conf	Term	J	Energy	Lifetime*
$3p^2 3d$	$(^3P)^4F$	9/2	695.151	9.62(-2)
		7/2	692.353	9.72(-2)
		5/2	690.059	9.82(-2)
		3/2	688.395	9.94(-2)
	$(^3P)^4D$	7/2	707.849	8.77(-2)
		5/2	705.826	8.69(-2)
		3/2	705.338	8.47(-2)
		1/2	706.854	7.27(-2)
	$(^3P)^4P$	5/2	741.257	2.53(-2)
		3/2	741.485	2.27(-2)
		1/2	741.791	2.10(-2)
	$(^3P)^2F$	7/2	789.539	2.24(-2)
		5/2	787.566	2.24(-2)
	$(^3P)^2D$	5/2	828.647	2.01(-2)
		3/2	831.737	2.01(-2)
	$(^3P)^2P$	3/2	698.335	6.62(-2)
		1/2	701.637	7.38(-2)
	$(^1D)^2G$	9/2	725.530	3.13(-1)
		7/2	724.640	3.08(-1)
	$(^1D)^2F$	7/2	683.638	2.54(-1)
		5/2	680.824	2.86(-1)
	$(^1D)^2D$	5/2	736.513	2.75(-2)
		3/2	738.275	3.00(-2)
	$(^1D)^2P$	3/2	764.889	3.99(-2)
		1/2	762.849	3.87(-2)
	$(^1D)^2S$	1/2	774.414	4.10(-2)
	$(^1S)^2D$	5/2	778.899	7.23(-2)
		3/2	773.422	6.66(-2)
$3s3d^2$	^4F	9/2	805.837	2.82(-2)
		7/2	805.439	2.78(-2)
		5/2	805.127	2.74(-2)
		3/2	804.905	2.72(-2)
	^4P	5/2	827.999	2.32(-2)
		3/2	827.777	2.29(-2)
		1/2	827.636	2.29(-2)
	^2G	9/2	866.628	3.43(-2)
		7/2	866.570	3.47(-2)
	^2F	7/2	900.996	1.80(-2)
		5/2	900.778	1.77(-2)
	^2D	5/2	862.825	1.96(-2)
		3/2	862.768	1.96(-2)
	^2P	3/2	926.437	1.36(-2)
		1/2	925.814	1.35(-2)
	^2S	1/2	914.173	1.68(-2)

*Figures in parentheses are the power of 10 by which the preceding number should be multiplied.

Table 12 Calculated reduced electric dipole radial integrals (in atomic units).

Transition		Reduced E1 integral
$3s^2 3p$	$- 3s3p^2$	(3s:R1:3p)= 0.8851
	$- 3s^2 3d$	(3p:R1:3d)= 1.1908
$3s3p^2$	$- 3p^3$	(3s:R1:3p)=-0.8838
	- 3s3p3d	(3p:R1:3d)=-1.1933
$3s^2 3d$	- 3s3p3d	(3s:R1:3p)=-0.8853
$3p^3$	$- 3p^2 3d$	(3p:R1:3d)= 1.1931
3s3p3d	$- 3p^2 3d$	(3s:R1:3p)= 0.8851
	$- 3s3d^2$	(3p:R1:3d)= 1.1973

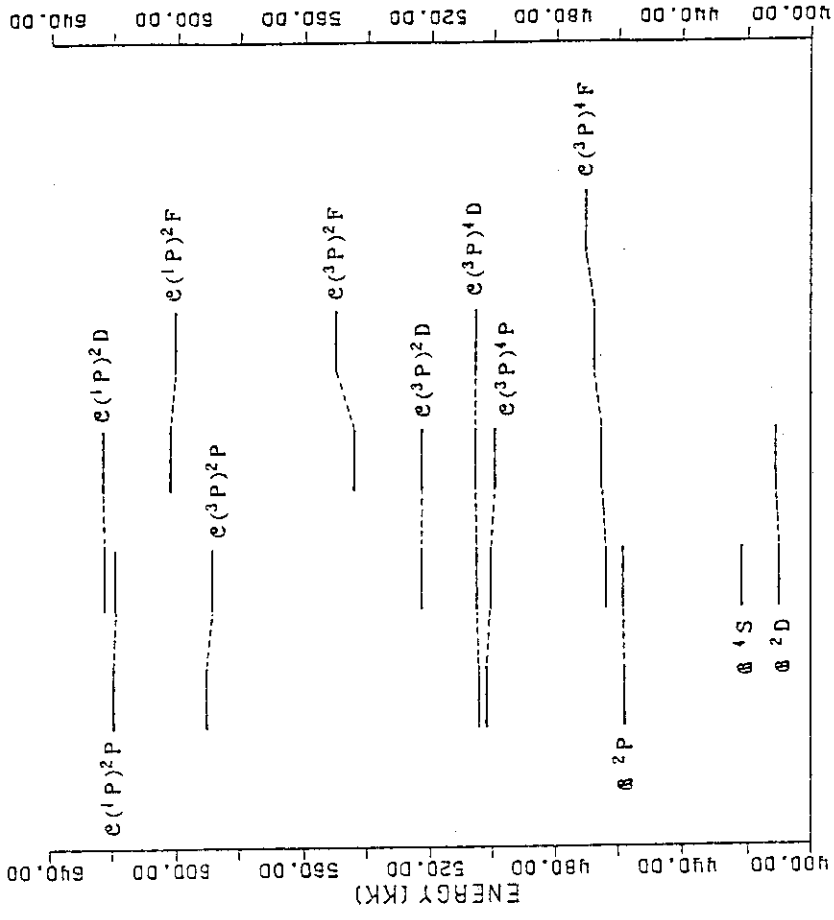

Fig.1 Calculated energy level diagram of $3p^3$ (a) and $3s3p3d$ (e) configurations of the first parity. Energy is in $10^3 cm^{-1}$.

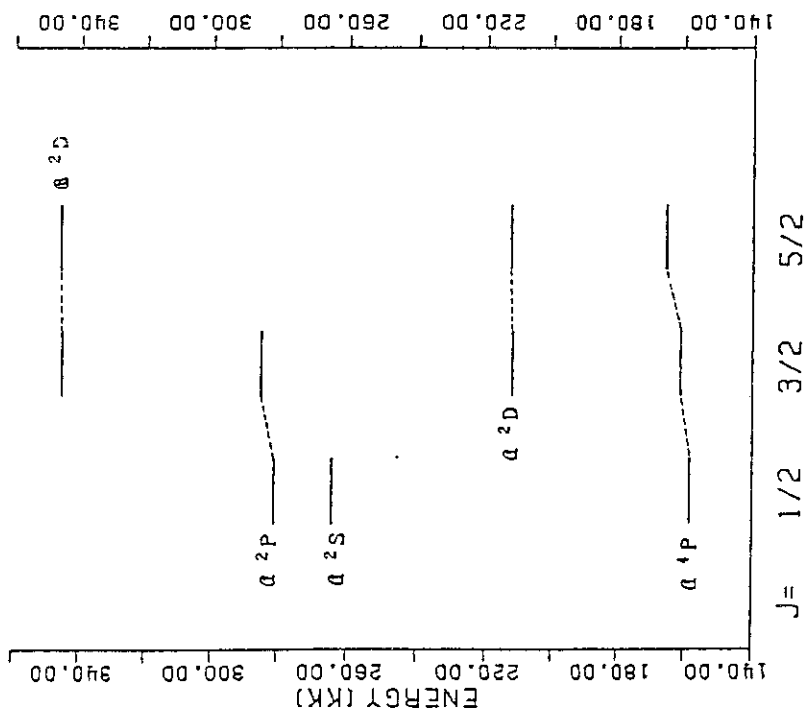

Fig.2 Calculated energy level diagram of $3s3p^2$ (a) and $3s^23d$ (e) configurations of the second parity.

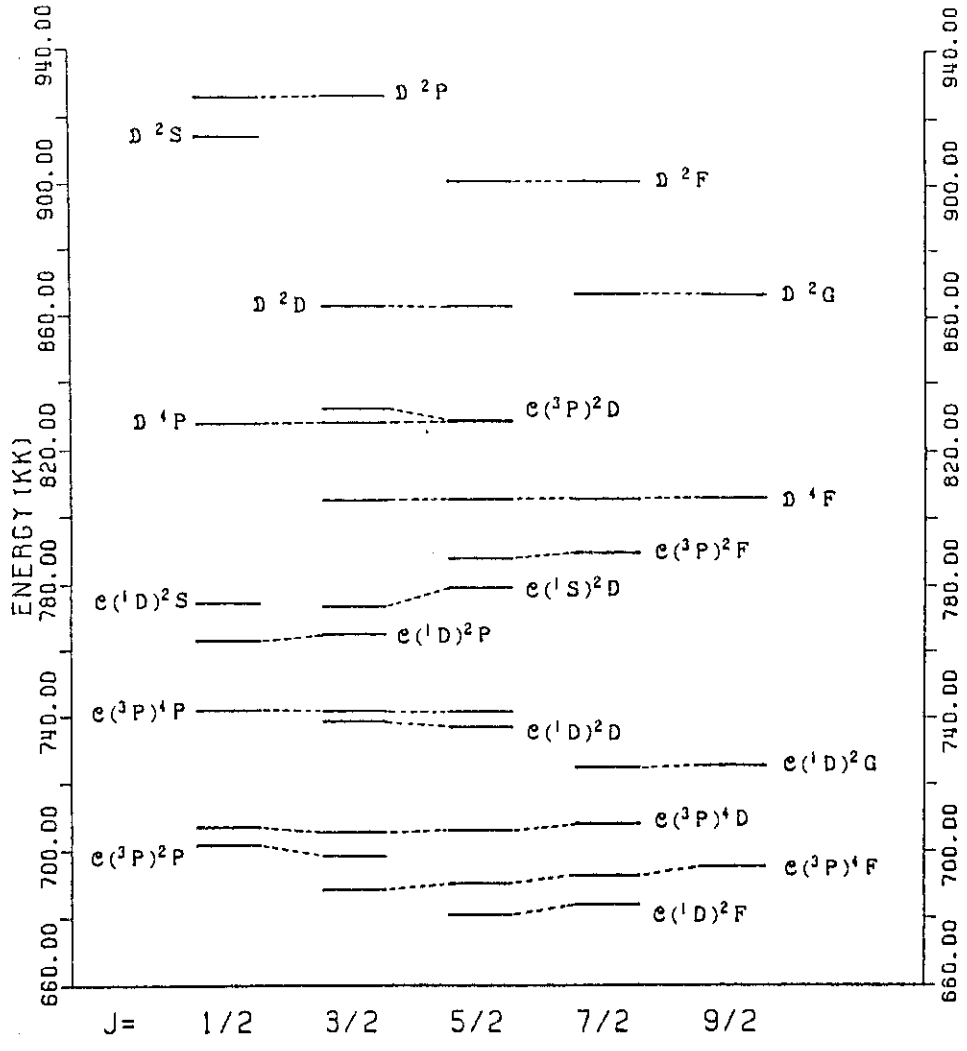

Fig.3 Calculated energy level diagram of $3p^3 3d$(e) and $3s^2 3d$(o) configurations of the second parity.

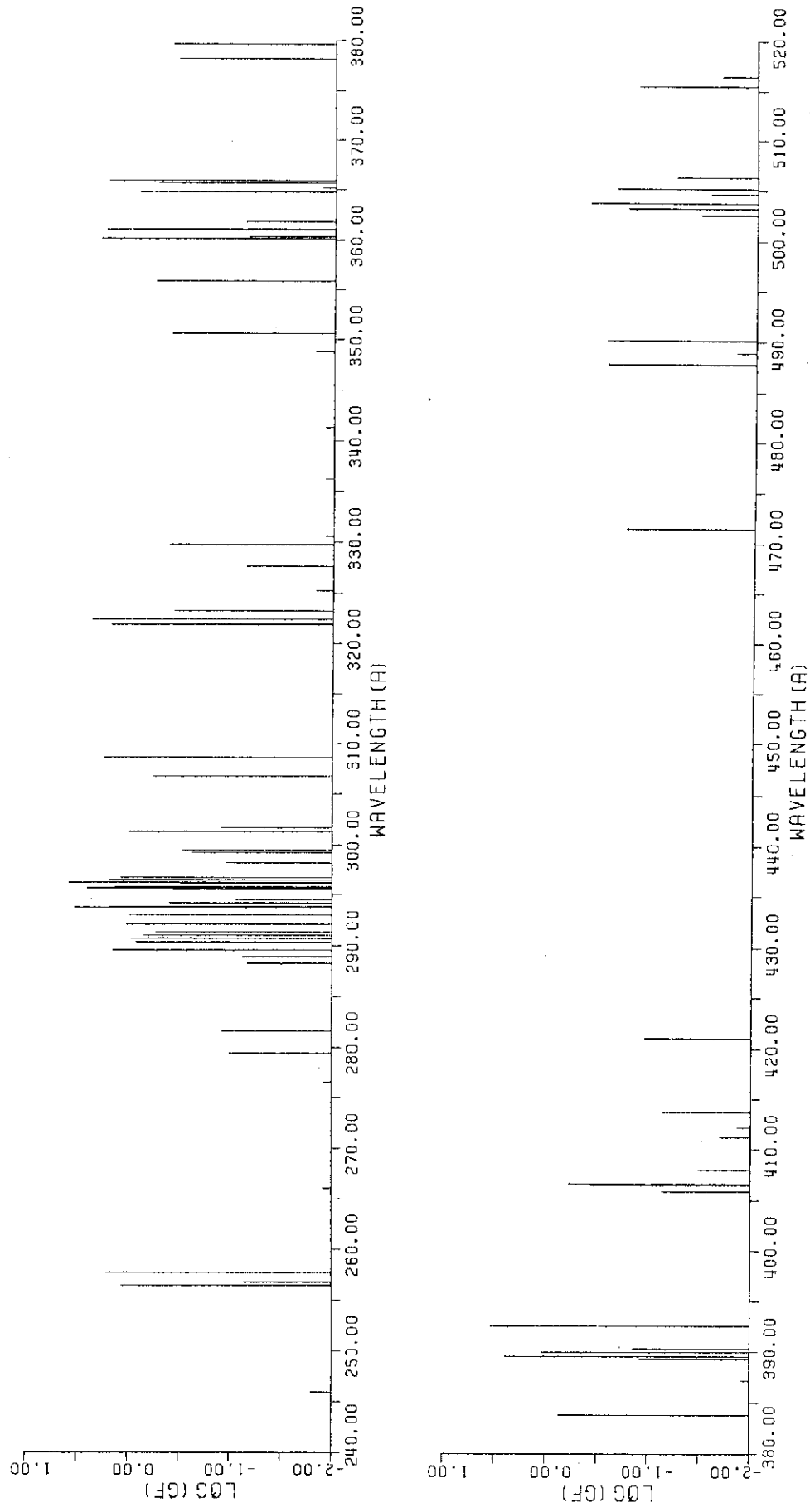

Fig.4 Calculated line pattern for the transitions in Ti X, corresponding to Table 10. (upper) 240–380Å and (lower) 380–520Å .

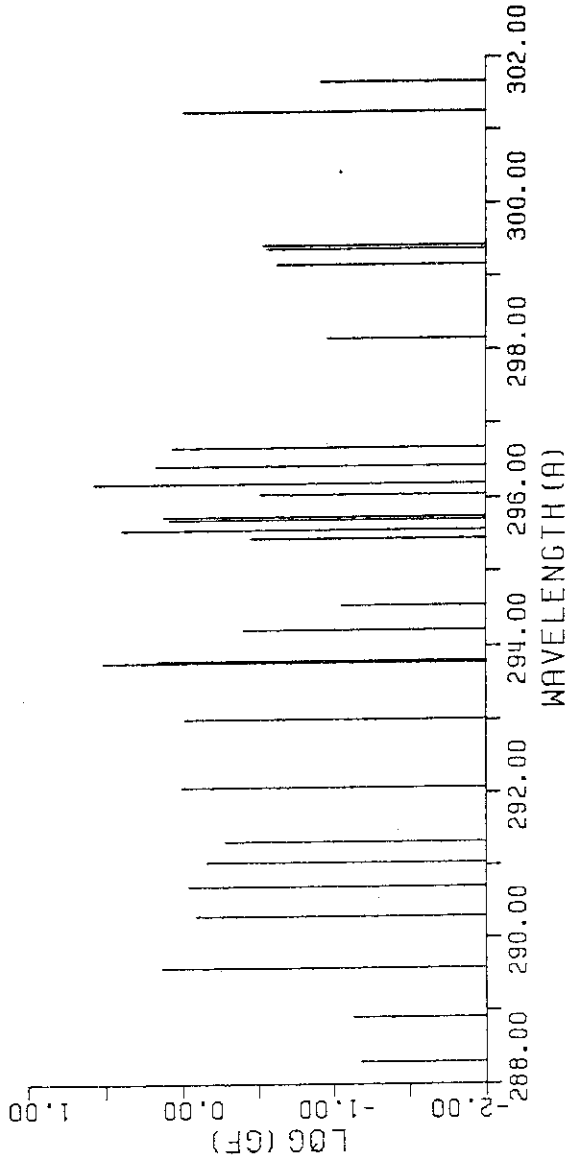

Fig.5 Enlarged partial line pattern in the wavelength range 288 to 302A .